State Observers for Mechatronics Systems with Rigid and Flexible Drive Dynamics

Alexandra-Iulia Szedlak-Stinean, Radu-Emil Precup and Radu-Codrut David
Department of Automation and Applied Informatics, Politehnica University of Timisoara, Bd. V. Parvan 2, 300223, Timisoara, Romania

Keywords: State Observers, Electromechanical Plant, Experimental Results, Rigid Drive Dynamics, Flexible Drive Dynamics, Adjustable Moment of Inertia.

Abstract: The mechatronics systems with rigid and flexible drive dynamics are nonlinear and complex processes. This paper proposes a controller with a novel structure, which is composed of three subsystems: a subsystem that provides the desired output and from the reference input a feed-forward signal, an observer and a feedback derived from the estimated states. This structure has the advantage that the response to reference signals can be decoupled from the response to disturbances. This paper also proposes observers based on predictive feedback, characterized by fast convergence and small sensitivity of the estimation to parameter variations. Design approaches for the controller and state observers are offered. The experimental setup considered in this paper, namely the Model 220 Industrial Plant Emulator (MIPE220), illustrates how the use of several control structures can be made accessible, easily understandable and increasingly attractive. The proposed design approaches are tested and validated in terms of conducting real-time experiments in terms of two experimental scenarios – step and staircase reference inputs – obtained for three specific values of the moment of inertia of the load disk.

1 INTRODUCTION

Mechatronics systems have experienced a fast and complex multidisciplinary development as a result of advances in various fields of applications such as (Isermann, 2005; Bishop, 2007; Gutiérrez-Carvajal et al., 2016): expert systems, automotive engineering, robotics and automation, structural dynamic systems, machine vision, control systems, servo mechanics, numerical computing systems based on microelectronics with a high degree of integration, consumer products, medical imaging systems, mobile apps, computer-aided and integrated manufacturing systems, transportation and vehicular systems, etc.

The development of linear and nonlinear observers has led over the years to a novel stage of engineering design. Luenberger was the first to introduce and solve the problem of designing observers for linear control systems (Luenberger, 1966). One of the central problems in control systems literature, designing observers for nonlinear control systems, was proposed in (Thau, 1973). In the hypothesis of linearity of the process model, the basic structure of the observer is always the same, but its realization will depend on the chosen context: continuous or discreet, deterministic or stochastic. An observer is very useful for implementing feedback stabilization or feedback regulation due to the fact that it is essentially an estimator for the state of the system, and some representative papers on this subject are (Brown and Hwang, 1996; Aghannan and Rouchon, 2003). The development of suitable algorithms to perform the estimation has been the focus of many researchers' attention and for this purpose, in order to estimate state variables from the available measurements, several techniques have been developed and introduced (Brown and Hwang, 1996; Aghannan and Rouchon, 2003; Marx et al., 2007; Lendek et al., 2008; Spurgeon, 2008; Magnis and Petit, 2016). In this context, the paper proposes a controller that can be considered as composed of three subsystems: a subsystem that provides the desired output and from the reference value a feed-forward signal, an observer and a feedback derived from the estimated states. The interesting structure of the controller allows it to be applied for a wide range of design methods. The controller structure and the forms of the equations are exactly the same for

Szedlak-Stinean, A., Precup, R. and David, R.
State Observers for Mechatronics Systems with Rigid and Flexible Drive Dynamics.
DOI: 10.5220/0007921203870394
In *Proceedings of the 16th International Conference on Informatics in Control, Automation and Robotics (ICINCO 2019)*, pages 387-394
ISBN: 978-989-758-380-3

systems with one input and one output as well as for systems with multiple inputs and outputs. The same controller structure can be obtained by employing many other design techniques. The defining feature of a state feedback controller and an observer have is the complexity of the controlled system that determines controller's complexity. As such a system model is actually contained by the controller. Thereby the internal model principle that prescribes that an internal model of the controlled system should be contained in the controller is in this paper exemplified.

This paper offers the next five contributions over the literature: 1. development of the dynamic equations used in the process mathematical models (MMs) of MIPE220 with rigid and flexible drive dynamics and the interpretation of these MMs as benchmark type models, 2. design approaches and implementation of state observers in three case studies dedicated to the position control of MIPE220 with rigid and flexible drive dynamics, 3. development of Matlab/Simulink programs to test the new control system structures, 4. experimental validation of proposed techniques, and 5. a comparative analysis of all design approaches for two experimental scenarios to highlight how the specified control system performance is achieved.

The paper discusses the following topics: the dynamic equations that characterize the electromechanical subsystem with rigid and flexible drive dynamics are pointed out in Section 2. Numerical values related to the MIPE220 are also given in Section 2. The proposed design approaches for the position control of a mechatronics system are discussed in Section 3. Section 4 presents experimental results concerning the implementation of the developed design approaches and also a comparative analysis of all control solutions. The main conclusions are highlighted in Section 5.

2 DYNAMIC EQUATIONS AND NUMERICAL VALUES FOR THE ELECTROMECHANICAL SUBSYSTEM MIPE220

The structure of the mechatronics application that represents the controlled process (MIPE220) is presented in Figure 1. The dynamic equations that describe the mechatronics system in case of rigid (a) and flexible (b) drive dynamics, considering θ_1 as the process output are:

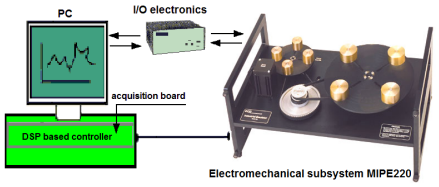

Figure 1: MIPE220 laboratory equipment.

$$\begin{aligned} &a)\ J_{dr}\ddot{\theta}_1+(c_1+c_2g^{-2})\dot{\theta}_1=T_D,\\ &b)\ J_{dr}\ddot{\theta}_1+(c_1+c_{12}g^{-2})\dot{\theta}_1-c_{12}g^{-1}\dot{\theta}_2+k(g^{-2}\theta_1-g^{-1}\theta_2)=T_D,\\ &\quad J_l\ddot{\theta}_2+(c_2+c_{12})\dot{\theta}_2-c_{12}g^{-1}\dot{\theta}_1+k(\theta_2-g^{-1}\theta_1)=0. \end{aligned} \tag{1}$$

with J_{dr}, J_d, J_l, J_p, g and g' expressed as

$$\begin{aligned} &J_{dr}=J_d+J_pg'^{-2}+J_lg^{-2},\ J_d=J_{ddr}+J_{wdr},\\ &J_p=J_{pdr}+J_{pld}+J_{backlash},\ J_l=J_{dld}+J_{wld},\\ &g=6n_{pd}/n_{pl},\ g'=n_{pd}/12. \end{aligned} \tag{2}$$

where J_{dr} – total inertia reflected to the drive disk, J_p, J_d, J_l, – pulley, drive disk and load disk inertia, c_1, c_2 – the drive and load friction, g, g' – drive gear and partial gear system ratio, θ_1, θ_2, θ_p – drive disk, load disk and idler pulleys positions where $\theta_1=g\theta_2$ or $\theta_1=g'\theta_p$.

2.1 Rigid Drive Dynamics

The first principle equations that describe the system in case of rigid drive dynamics are (ECP, 2010; Szedlak-Stinean et al., 2016):

$$\begin{cases} \dot{x}_1=x_2,\\ \dot{x}_2=\dfrac{-(c_1+c_2g^{-2})x_2}{J_d+J_pg'^{-2}+J_lg^{-2}}+\dfrac{T_D}{J_d+J_pg'^{-2}+J_dg^{-2}},\\ y=x_1. \end{cases} \tag{3}$$

The state-space MM (SS-MM) of MIPE220 with rigid drive dynamics is

$$\begin{bmatrix}\dot{x}_1\\ \dot{x}_2\end{bmatrix}=\begin{bmatrix}0 & 1\\ 0 & \dfrac{-(c_1+c_2g^{-2})}{J_d+J_pg'^{-2}+J_lg^2}\end{bmatrix}\begin{bmatrix}x_1\\ x_2\end{bmatrix}+\begin{bmatrix}0\\ \dfrac{1}{J_d+J_pg'^{-2}+J_lg^2}\end{bmatrix}T_D, \tag{4}$$

$$y=[1\quad 0][x_1\quad x_2]^T.$$

where T_D is the drive torque ($T_D=u$), $\mathbf{x}=[x_1\ \ x_2]^T=[\theta_1\ \ d\theta_1/dt]^T$ is the state vector (T indicates matrix transposition) and y is the output. Considering zero initial conditions, the application of the Laplace transform to (1a)) leads to the following transfer function (t.f.):

$$\frac{\theta_1(s)}{T_D(s)}=\frac{1/(\mathrm{J_d}+\mathrm{J_p g^{r\text{-}2}}+\mathrm{J_l g^2})}{s[s+(c_1+c_2 g^{-2})/(\mathrm{J_d}+\mathrm{J_p g^{r\text{-}2}}+\mathrm{J_l g^2})]}, \quad (5)$$

Using (4) and (5) the matrices **A**, **B** and **C** related to the SS-MM and the t.f.s for three significant values of the moment of inertia of the load disk are given in Table 1 (ECP, 2010; Szedlak-Stinean et al., 2016).

Table 1: SS-MM matrices and transfer functions expressions of MIPE220 with rigid drive dynamics.

Inertia	Matrices **A**, **B** and **C**	Process transfer function $\theta_1(s)/T_D(s)$
J_{l_1}	$\mathbf{A}=\begin{bmatrix}0 & 1\\ 0 & -8.63\end{bmatrix},\mathbf{B}=\begin{bmatrix}0\\ 7036\end{bmatrix},\mathbf{C}=\begin{bmatrix}1 & 0\end{bmatrix}$	$\frac{7036}{s(s+8.63)}$
J_{l_2}	$\mathbf{A}=\begin{bmatrix}0 & 1\\ 0 & -5.35\end{bmatrix},\mathbf{B}=\begin{bmatrix}0\\ 4362\end{bmatrix},\mathbf{C}=\begin{bmatrix}1 & 0\end{bmatrix}$	$\frac{4362}{s(s+5.35)}$
J_{l_3}	$\mathbf{A}=\begin{bmatrix}0 & 1\\ 0 & -3.37\end{bmatrix},\mathbf{B}=\begin{bmatrix}0\\ 2741\end{bmatrix},\mathbf{C}=\begin{bmatrix}1 & 0\end{bmatrix}$	$\frac{2741}{s(s+3.37)}$

2.2 Flexible Drive Dynamics

The first principle equations that describe the system in case of flexible drive dynamics are (ECP, 2010):

$$\begin{cases}\dot{x}_1=x_2,\\ \dot{x}_2=\dfrac{-(kg^{-2})x_1}{J_{dr}}+\dfrac{-(c_1+c_{12}g^{-2})x_2}{J_{dr}}+\dfrac{kg^{-1}}{J_{dr}}+\dfrac{c_{12}g^{-1}}{J_{dr}},\\ \dot{x}_3=x_4,\\ \dot{x}_4=\dfrac{(kg^{-1})x_1}{J_l}+\dfrac{(c_{12}g^{-1})x_2}{J_l}+\dfrac{(-k)x_3}{J_l}+\dfrac{-(c_2+c_{12})x_4}{J_l},\\ y=x_1.\end{cases} \quad (6)$$

The SS-MM of MIPE220 with flexible drive dynamics is

$$\begin{bmatrix}\dot{x}_1\\ \dot{x}_2\\ \dot{x}_3\\ \dot{x}_4\end{bmatrix}=\begin{bmatrix}0 & 1 & 0 & 0\\ \frac{-(kg^{-2})}{J_{dr}} & \frac{-(c_1+c_1g^{-2})}{J_{dr}} & \frac{kg^{-1}}{J_{dr}} & \frac{c_1g^{-1}}{J_{dr}}\\ 0 & 0 & 0 & 1\\ \frac{kg^{-1}}{J_l} & \frac{c_1g^{-1}}{J_l} & \frac{-k}{J_l} & \frac{-(c_2+c_{12})}{J_l}\end{bmatrix}\begin{bmatrix}x_1\\ x_2\\ x_3\\ x_4\end{bmatrix}+\begin{bmatrix}0\\ \frac{1}{\mathrm{J_d}+\mathrm{J_p g^{r\text{-}2}}+\mathrm{J_l g^2}}\\ 0\\ 0\end{bmatrix}T_D,$$
$$y=[1\ 0\ 0\ 0][x_1\ x_2\ x_3\ x_4]^T. \quad (7)$$

where T_D is the drive torque ($T_D=u$, u is the input), $\mathbf{x}=[x_1\,x_2\,x_3\,x_4]^T=[\theta_1\,d\theta_1/dt\,\theta_2\,d\theta_2/dt]^T$ is the state vector and y is the output. The following t.f. is attached to (7):

$$\frac{\theta_1(s)}{T_D(s)}=\frac{J_l s^2+(c_2+c_{12})s+k}{d_4 s^4+d_3 s^3+d_2 s^2+d_1 s}, \quad (8)$$

where $d_4=J_{dr}J_l$, $d_3=J_{dr}(c_2+c_{12})+J_l(c_1+c_{12}/g^2)$, $d_2=J_{dr}k+J_lk/g^2+c_1c_2+c_1c_{12}+c_{12}c_2/g^2$, $d_1=c_1k+c_2k/g^2$. Using (7) and (8) the matrices **A**, **B** and **C** and the t.f.s. related to MIPE220 with flexible drive dynamics for three values of the moment of inertia of the load disk are given in Table 2 (ECP, 2010; Szedlak-Stinean et al., 2017).

2.3 MIPE220 Parameters Values

For the development of the proposed design approaches, the parameter values for the electromechanical subsystem, as presented in the manual (ECP, 2010), are shown in Table 3.

Due to the fact that the employed laboratory equipment does not permit a continuous variation of the moment of inertia, the suggested control solutions which will be tested and validated through experiments are designed for three specific load disk inertia values, J_{li}, $i\in\{1,2,3\}$ (ECP, 2010; Szedlak-Stinean et al., 2016; Szedlak-Stinean et al., 2017): the low value J_{l1}=0.0065kgm^2 (load disk without any weights on it), the middle value J_{l2}=0.01474kgm^2 (load disk has four 0.2 kg weights on it) and the high value J_{l3}=0.0271kgm^2 (load disk has four 0.5 kg weights on it).

3 STATE FEEDBACK AND OBSERVER-BASED CONTROLLER DESIGN

In cases where the process states are not accessible for measurements or are only partially accessible for measurements and if the process is observable, then it is possible to estimate its states. For this purpose, state estimators or state observers are utilized. The observability test of the linearized SS-MMs (4) and (7) can be done using the matrix

$$\mathbf{Q}_o=[C^T\ \ C^TA\ \ C^T\mathbf{A^2}\ \ C^T\mathbf{A^3}\ \ C^T\mathbf{A^4}...]^T. \quad (9)$$

The numerical values specific to the analyzed mechatronics application given in Tables 1 and 2 are used in the computation of the rank of $\mathbf{Q}_o$.

The starting point in order to specify the relations that describe the functioning of a state observer, is the SS-MM corresponding to the process, assumed known, with the form

$$\begin{aligned}\dot{\mathbf{x}}&=\mathbf{A}\,\mathbf{x}+\mathbf{B}\,u,\\ y&=\mathbf{C}\,\mathbf{x}.\end{aligned} \quad (10)$$

Table 2: SS-MM matrices and transfer functions expressions for MIPE220 with flexible drive dynamics.

Inertia	Matrices **A**, **B** and **C**	Process transfer function $\theta_1(s)/T_D(s)$
J_{l_1}	$\mathbf{A}=\begin{bmatrix}0 & 1 & 0 & 0\\ -1259 & -12.068 & 5036 & 10.13\\ 0 & 0 & 0 & 1\\ 325 & 0.654 & -1300 & -10.307\end{bmatrix}, \mathbf{B}=\begin{bmatrix}0\\ 13850\\ 0\\ 0\end{bmatrix}, \mathbf{C}=[1\ \ 0\ \ 0\ \ 0]$	$\frac{13850\,(s^2+10.307s+1300)}{s(s^3+22.37s^2+2677.2s+22078)}$
J_{l_2}	$\mathbf{A}=\begin{bmatrix}0 & 1 & 0 & 0\\ -1259 & -12.068 & 5036 & 10.13\\ 0 & 0 & 0 & 1\\ 145 & 0.3 & -579 & -4.59\end{bmatrix}, \mathbf{B}=\begin{bmatrix}0\\ 13850\\ 0\\ 0\end{bmatrix}, C=\begin{bmatrix}1 & 0 & 0 & 0\end{bmatrix}$	$\frac{13850\,(s^2+4.59s+579)}{s(s^3+16.65s^2+1893.7s+9827.4)}$
J_{l_3}	$\mathbf{A}=\begin{bmatrix}0 & 1 & 0 & 0\\ -1259 & -12.068 & 5036 & 10.13\\ 0 & 0 & 0 & 1\\ 77.9 & 0.157 & -312 & -2.47\end{bmatrix}, \mathbf{B}=\begin{bmatrix}0\\ 13850\\ 0\\ 0\end{bmatrix}, \mathbf{C}=[1\ \ 0\ \ 0\ \ 0]$	$\frac{13850\,(s^2+2.47s+312)}{s(s^3+14.53s^2+1599.4s+5290.4)}$

Table 3: MIPE220 parameter values.

Electromechanical subsystem MIPE220 parameter values		
Parameters	Values	Remarks
J_{ddr}	0.00040 [kgm^2]	
J_{dld}	0.0065 [kgm^2]	
$J_{backlash}$	0.000031 [kgm^2]	
J_{wdr}	0.0021 [kgm^2]	4·0.2 kg at r_{wdr}=0.05 m
J_{wdr}	0.00561 [kgm^2]	4·0.5 kg at r_{wdr}=0.05 m
J_{wld}	0.00824 [kgm^2]	4·0.2 kg at r_{wld}=0.1 m
J_{wld}	0.0206 [kgm^2]	4·0.5 kg at r_{wld}=0.1 m
J_{pdr} or J_{pld}	0.000008 [kgm^2]	n_{pd}=24 or n_{pl}=24
J_{pdr} or J_{pld}	0.000039 [kgm^2]	n_{pd}=36 or n_{pl}=36
c_1	0.004 [Nm/rad/s]	
c_2	0.05 [Nm/rad/s]	
c_{12}	0.017 [Nm/rad/s]	
k	8.45 [Nm/rad]	

The variable that is the target of the control process is the output. Firstly, all components of the state vector are assumed as measured. The feedback is constrained to be linear, so it can be considered as (Åström and Murray, 2009)

$$u = -\mathbf{K}\,\mathbf{x} + K_{ref}\,r \tag{11}$$

where r is the reference input, K_{ref} is the feed-forward gain and **K** is the state feedback gain matrix. The state feedback gain matrix of MIPE220 with rigid (a) and flexible (b) drive dynamics are

$$\begin{aligned} &a)\ \ \mathbf{K}=[k_{c1}\quad k_{c2}],\\ &b)\ \ \mathbf{K}=[k_{c1}\quad k_{c2}\quad k_{c3}\quad k_{c4}]. \end{aligned} \tag{12}$$

The pole placement method is applied to compute **K** using three sets of imposed poles, each for three specific load disk inertia values, i.e., J_{l1}, J_{l2}, J_{l3}. The closed-loop system poles and the state feedback gain matrix parameter values are presented in Table 4. The closed loop system obtained when the feedback (11) is applied to the system (10) is given by

$$\dot{\mathbf{x}} = (\mathbf{A}-\mathbf{B}\,\mathbf{K})\mathbf{x} + \mathbf{B}\,K_{ref}\,r. \tag{13}$$

The SS-MM corresponding to the state observer has the same structure as the process (10) and is completed with a correction relation based on the output error $\tilde{y}=y-\hat{y}$. Consequently, the MM is rewritten in the form (Åström and Murray, 2009)

$$\begin{aligned} &\dot{\hat{\mathbf{x}}}=\mathbf{A}\hat{\mathbf{x}}+\mathbf{B}u+\mathbf{L}(y-\mathbf{C}\hat{\mathbf{x}})=(\mathbf{A}-\mathbf{L}\mathbf{C})\hat{\mathbf{x}}+\mathbf{B}u+\mathbf{L}y,\\ &\hat{y}=\mathbf{C}\hat{\mathbf{x}}, \end{aligned} \tag{14}$$

where **L** is the observer gain. The parameters of the observer gain for MIPE220 with rigid (a) and flexible (b) drive dynamics are

$$\begin{aligned} &a)\ \ \mathbf{L}=[l_1\quad l_2]^T,\\ &b)\ \ \mathbf{L}=[l_1\quad l_2\quad l_3\quad l_4]^T. \end{aligned} \tag{15}$$

In order to analyze the observer, the state estimation error is defined as $\tilde{\mathbf{x}}=\mathbf{x}-\hat{\mathbf{x}}$. Differentiating and replacing the expressions of $\dot{\tilde{\mathbf{x}}}$ and $\hat{\mathbf{x}}$ leads to $\dot{\tilde{x}}=(A-LC)\tilde{x}$. The error $\tilde{\mathbf{x}}$ will go to zero if the matrix **L** is chosen such that the matrix $(\mathbf{A}-\mathbf{L}\mathbf{C})$ has eigenvalues / poles with negative real parts. The appropriate selection of the eigenvalues / poles determines the convergence rate (Åström and Murray, 2009). Taking this into account, the design of the state observer involves solving a poles placement problem and also calculating the parameters of the observer gain. The starting point in designing the state observer is the expression of the characteristic polynomial

$$\begin{aligned} \Delta_{ob}(s) &= \det(s\,\mathrm{I}-\mathrm{A}+\mathrm{L}\,\mathrm{C})\\ &= s^n+\alpha_{n-1}s^{n-1}+\ldots+\alpha_1 s+\alpha_0. \end{aligned} \tag{16}$$

Table 4: Selected poles and state feedback gain matrix parameter values.

J_{l_i}	Rigid drive dynamics				Flexible drive dynamics							
	Selected poles		State feedback gain matrix		Selected poles				State feedback gain matrix			
	p_1^*	p_2^*	k_{c1}	k_{c2}	p_1^*	p_2^*	p_3^*	p_4^*	k_{c1}	k_{c2}	k_{c3}	k_{c4}
J_{l_1}	-20	-11	0.0313	0.0032	-12.26	-48.49	-28.32+59.33i	-28.32-59.33i	0.3234	0.0069	-0.7223	0.0247
J_{l_2}	-20	-7	0.0321	0.005	-8.33	-26.32	-17.52+38.48i	-17.52-38.48i	0.0749	0.0038	-0.103	0.0124
J_{l_3}	-20	-5	0.0365	0.0079	-4.95	-16.46	-17.38+31.37i	-17.38-31.37i	0.028	0.003	-0.015	0.0104

Table 5: Selected poles for the observer and observer gain parameter values.

J_{l_i}	Rigid drive dynamics				Flexible drive dynamics							
	Selected poles		Observer gain matrix		Selected poles				Observer gain matrix			
	p_{o1}	p_{o2}	l_1	l_2	p_{o1}	p_{o2}	p_{o3}	p_{o4}	l_1	l_2	l_3	l_4
J_{l_1}	-220	-121	332.37	23751.6	-36.80	-145.47	-84.96+177.9i	-84.96-177.9i	329.8	65168.8	1331	13480.37
J_{l_2}	-220	-77	291.65	15379.7	-25.06	-78.79	-52.56+115.4i	-52.56-115.4i	192.3	23871.9	320.4	2252.13
J_{l_3}	-220	-55	271.63	11184.6	-14.83	-49.46	-52.16+94.12i	-52.16-94.12i	154.1	15181.1	143.3	390.83

By allocating the poles of the observer, the characteristic polynomial $\Delta_{ob}(s)$ is expressed as

$$\Delta_{ob}(s) = \prod(s - p_{ov}) = s^n + \beta_{n-1}s^{n-1} \ldots + \beta_0 \quad (17)$$

The selected poles for the observer and observer gain matrix parameter values are given in Table 5.

Because both the system (10) and the observer (14) have the same order n, the order of the closed loop system is $2n$. In order to obtain the state feedback observer, the design of the observer as well as the design of the state feedback can be realized separately. The closed-loop system is defined as

$$\begin{bmatrix} \dot{\mathbf{x}} \\ \dot{\tilde{\mathbf{x}}} \end{bmatrix} = \begin{bmatrix} \mathbf{A} - \mathbf{B}\,\mathbf{K} & \mathbf{B}\,\mathbf{K} \\ 0 & \mathbf{A} - \mathbf{L}\,\mathbf{C} \end{bmatrix} \begin{bmatrix} \mathbf{x} \\ \tilde{\mathbf{x}} \end{bmatrix} + \begin{bmatrix} \mathbf{B}\,K_{ref} \\ 0 \end{bmatrix} r \quad (18)$$

Due to the fact that the matrix on the right side is block diagonal, the characteristic polynomial of the closed-loop system has the form

$$\Delta_{xx}(s) = \det(s\,\mathbf{I} - \mathbf{A} + \mathbf{B}\,\mathbf{K}) \det(s\,\mathbf{I} - \mathbf{A} + \mathbf{L}\,\mathbf{C}). \quad (19)$$

This property is called the separation principle (Åström and Murray, 2009). A schematic diagram of the controller is illustrated in Figure 2. It can be observed that the controller includes a dynamic model of the plant, thus respecting the internal model principle. It can also be noticed that the observer determines the dynamics of the controller. As such, the controller can be regarded as a dynamical system having y as input and u as output:

$$\begin{aligned} \dot{\hat{\mathbf{x}}} &= (\mathbf{A} - \mathbf{B}\,\mathbf{K} - \mathbf{L}\,\mathbf{C})\hat{\mathbf{x}} + \mathbf{L}\,y, \\ u &= -\mathbf{K}\,\hat{\mathbf{x}} + K_{ref}\,r. \end{aligned} \quad (20)$$

The t.f. of the controller has the form

$$H_c(s) = \mathbf{K}\left[s\,\mathbf{I} - \mathbf{A} + \mathbf{B}\,\mathbf{K} + \mathbf{L}\,\mathbf{C}\right]^{-1}\mathbf{L}. \quad (21)$$

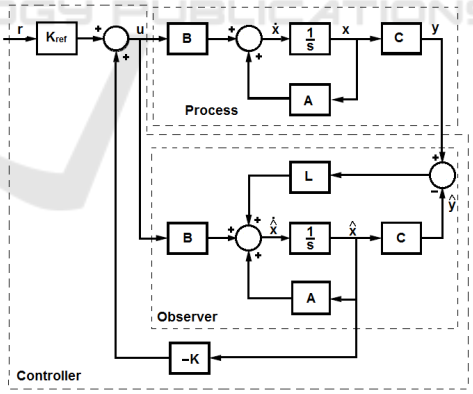

Figure 2: Schematic diagram of an observer-based controller.

4 EXPERIMENTAL RESULTS

The observer-based controller structure was developed and tested on the mechatronics system – MIPE220 – with rigid and flexible drive dynamics, in the framework of position control solutions designed

Table 6: Mean Square errors.

Inertia	Rigid drive dynamics				Flexible drive dynamics			
	ref_{step}		$ref_{staircase}$		ref_{step}		$ref_{staircase}$	
	Sim	*Exp*	*Sim*	*Exp*	*Sim*	*Exp*	*Sim*	*Exp*
J_{l_1}	5.5161e-06	0.0035	2.2754e-06	0.0014	3.4579e-05	0.0244	1.2967e-05	0.0128
J_{l_2}	5.3035e-05	0.0041	2.0467e-05	0.0018	6.1088e-04	0.0255	1.6291e-04	0.0137
J_{l_3}	4.0919e-04	0.0059	1.5566e-04	0.0022	3.5115e-03	0.0737	1.3168e-03	0.0401

for three specific load disk inertia values. The proposed design approaches were tested and validated by real-time experimental results. The system's responses in two experimental scenarios were considered: 1. the proposed control solutions responses were tested first using a step reference and are illustrated in Figures 3 and 5 and 2. a staircase change for the reference signal was employed and the proposed control solutions were tested again on the time frame of 30s and are illustrated in Figures 4 and 6.

In order to highlight how the specified control system performance was achieved, a comparative analysis between simulation and experimental results is carried out in terms of MSE values included in Table 6.The values of MSE, considered as a global performance index, between the real system variable p_k and its estimation $\hat{p}_k$, are defined as (p – position):

$$MSE = \frac{1}{m}\sum_{k=1}^{m}(p_k - \hat{p}_k)^2. \quad (22)$$

Taking into account the MSE values presented in Table 6 and the graphs illustrated in Figures 3 to 6, a set of following conclusions are pointed out: 1) the motivation to use observers (state observers) is due to the fact that through the predictive negative reaction, these design approaches have the advantage of faster convergence and a reduced sensitivity of estimation to parameter variation; 2) the controller structure is identical for systems with one input and one output as well as for systems with multiple inputs and outputs with the same form for the controller equations, the only difference being the fact that the feedback gain **K** and the observer gain **L** are matrices instead of vectors; 3) the separation principle – for the output feedback, the eigenvalue assignment can be split into an observer and a state feedback eigenvalue assignment – leads to a simplified design; 4) with one dynamic system both a controller and an observer can be developed; 5) the proposed approaches offer contributions for the robustness and dynamic performance of the system; 6) based on the comparative analysis it can be concluded that the proposed design approaches, prove to be viable and ensure a good reference tracking ability; 7) the use of these state observers leads to dynamically and permanently improved performance.

5 CONCLUSIONS

This paper gives details regarding the design and implementation of state observers designed for three specific load disk inertia values in order to estimate the position for a mechatronics system with rigid and flexible drive dynamics. The proposed design approaches are validated by means of real-time experimental results. The graphs illustrated in Figures 3 to 6 proved that these approaches are viable and ensure a good reference tracking ability. The use of these observers leads to dynamically and permanently improved performance.

Future work will investigate further improvements of the performance indices for the proposed design approaches. Additionally, optimal parameter tuning will replace the pole placement method. Further work will also aim to adapt these observers to other important cases, through the extension of the approaches suggested in this paper to other illustrative applications that include robotics and autonomous systems (Blažič, 2014; Kovács et al., 2016), fuzzy models and control (Precup et al., 2018), engines (Andoga et al., 2018), cognitive models for prediction and control (Direito et al., 2017; Ferreira et al., 2017; Braga et al., 2019).

ACKNOWLEDGEMENTS

This work was supported by grants from the Ministry of Research and Innovation, CNCS - UEFISCDI, project numbers PN-III-P1-1.1-PD-2016-0331 and PN-III-P1-1.1-PD-2016-0683, within PNCDI III.

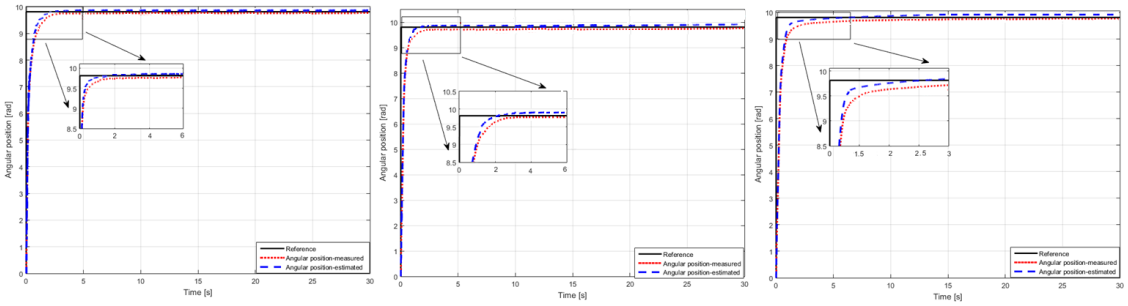

Figure 3: Experimental results concerning the behaviour of observer-based controller designed for MIPE220 with rigid drive dynamics (step reference): case study 1, 2 and 3.

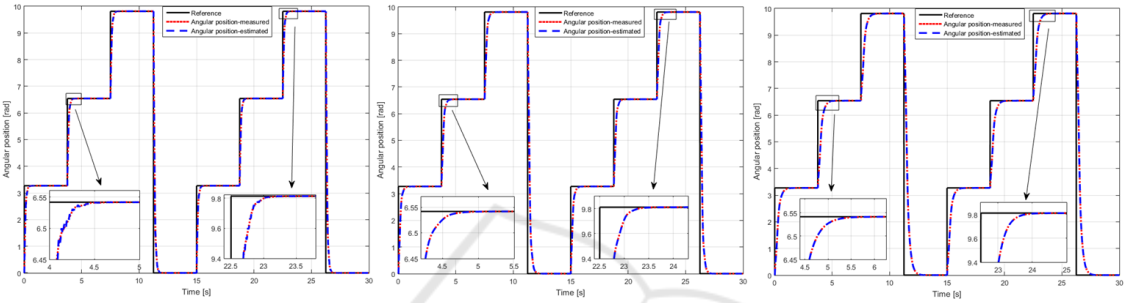

Figure 4: Experimental results concerning the behaviour of observer-based controller designed for MIPE220 with rigid drive dynamics (staircase reference): case study 1, 2 and 3.

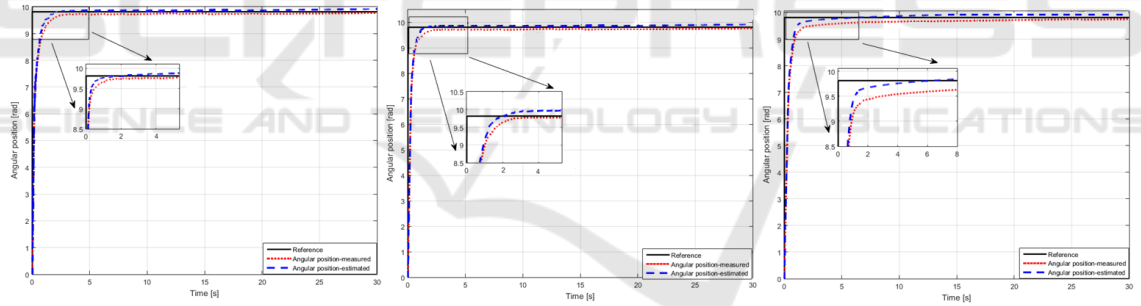

Figure 5: Experimental results concerning the behaviour of observer-based controller designed for MIPE220 with flexible drive dynamics (step reference): case study 1, 2 and 3.

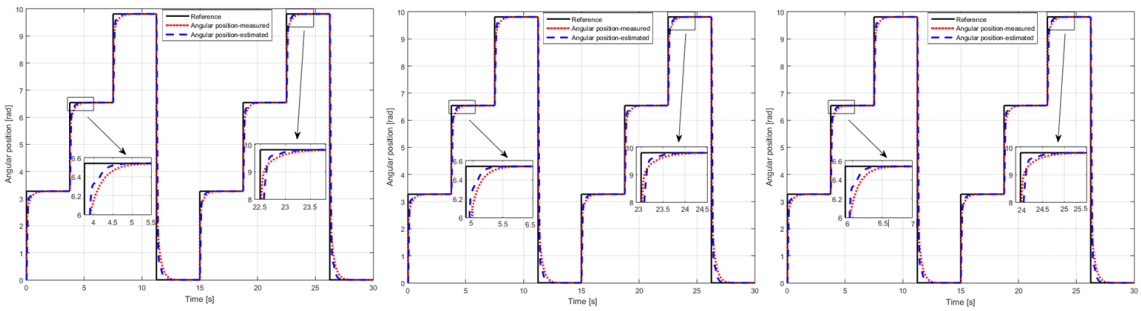

Figure 6: Experimental results concerning the behaviour of observer-based controller designed for MIPE220 with flexible drive dynamics (staircase reference): case study 1, 2 and 3.

REFERENCES

Aghannan, N., Rouchon, P., 2003. An intrinsic observer for a class of Lagrangian systems. *IEEE Transactions on Automatic Control.* 48, 936-945.

Andoga, R., Főző, L., Judičák, J., Bréda, R., Szabo, S., Rozenberg, R., Džunda, M., 2018. Intelligent situational control of small turbojet engines. *International Journal of Aerospace Engineering*. 2018, paper 8328792, 1-16.

Åström, K. J., Murray, R. M., 2009. *Feedback Systems. An introduction for scientists and engineers*. Princeton, New Jersey, Princeton University Press.

Bishop, R. H., 2007. *The Mechatronics Handbook*, 2nd ed. Boca Raton, FL: CRC Press.

Blažič, S., 2014. On periodic control laws for mobile robots. *IEEE Transactions on Industrial Electronics*. 61 (7), 3660-3670.

Braga, D., Madureira, A. M., Coelho, L., Ajith, R., 2019. Automatic detection of Parkinson's disease based on acoustic analysis of speech. *Engineering Applications of Artificial Intelligence*. 77, 148-158.

Brown, R. G., Hwang, P. Y. C., 1996. *Introduction to Random Signals and Applied Kalman Filtering,* 3rd ed. New York: John Wiley & Sons.

Direito, B., Teixeira, C. A., Sales, F., Castelo-Branco, M., Dourado, A., 2017. A realistic seizure prediction study based on multiclass SVM. *International Journal of Neural Systems*. 27 (3), 1-15.

ECP, 2010. *Industrial Emulator/Servo Trainer Model 220 System, Testbed for Practical Control Training*. Bell Canyon, CA: Educational Control Products.

Ferreira, R., Graça Ruano, M., Ruano, A. E., 2017. Intelligent non-invasive modeling of ultrasound-induced temperature in tissue phantoms. *Biomedical Signal Processing and Control*. 33, 141-150.

Gutiérrez-Carvajal, R. E., de Melo, L. F., Rosário, J. M., Tenreiro Machado, J. A., 2016. Condition-based diagnosis of mechatronic systems using a fractional calculus approach. *International Journal of Systems Science*. 47, 2169-2177.

Isermann, R., 2005. *Mechatronic Systems: Fundamentals*. Berlin, Heidelberg, New York: Springer-Verlag.

Kovács, B., Szayer, G., Tajti, F., Burdelis, M., Korondi, P., 2016. A novel potential field method for path planning of mobile robots by adapting animal motion attributes. *Robotics and Autonomous Systems*. 82, 24-34.

Lendek, Z., Babuska, R., De Schutter, B., 2008. Distributed Kalman filtering for cascaded systems. *Engineering Applications of Artificial Intelligence*. 21, 457-469.

Luenberger, D. G., 1966. Observers for multivariable systems. *IEEE Transactions on Automatic Control.* 11, 190-197.

Magnis, L., Petit, N., 2016. Angular velocity nonlinear observer from single vector measurements. *IEEE Transanctions on Automatic Control*. 61, 2473-2483.

Marx, B., Koenig, D., Ragot, J., 2007. Design of observers for Takagi-Sugeno descriptor systems with unknown inputs and application to fault diagnosis. *IET Control Theory & Applications*. 1, 1487-1495.

Precup, R.-E., Teban, T.-A., Albu, A., Szedlak-Stinean, A.-I., Bojan-Dragos, C.-A., 2018. Experiments in incremental online identification of fuzzy models of finger dynamics. *Romanian Journal of Information Science and Technology*. 21 (4), 358-376.

Spurgeon, S. K., 2008. Sliding mode observers: A survey. *International Journal of Systems Science*. 39, 751-764.

Szedlak-Stinean, A.-I., Precup, R.-E. Preitl, S., Petriu, E. M., Bojan-Dragos, C.-A., 2016. State feedback control solutions for a mechatronics system with variable moment of inertia. In *Proc. 13th International Conference on Informatics in Control, Automation and Robotics*, Lisbon, Portugal, 458-465.

Szedlak-Stinean, A.-I., Precup, R.-E., Petriu, E. M., 2017. Fuzzy and 2-DOF controllers for processes with a discontinuously variable parameter. In *Proc. 14th International Conference on Informatics in Control, Automation and Robotics*, Madrid, Spain, 431-438.

Thau, F. E., 1973. Observing the state of nonlinear dynamic systems. *International Journal of Control*. 17, 471-479.